Contents lists available at ScienceDirect

Journal of Magnetism and Magnetic Materials

journal homepage: http://ees.elsevier.com

Research articles

A spin-wave magnetometer with a positive feedback

M. Balinskiy [a], H. Chiang [a], A. Kozhevnikov [b], Y. Filimonov [b,c], A.A. Balandin [a], A. Khitun [a,*]

[a] Department of Electrical and Computer Engineering, University of California – Riverside, Riverside, CA 92521, USA
[b] Kotelnikov Institute of Radio-Engineering and Electronics of the Russian Academy of Sciences, Saratov 410019, Russia
[c] Saratov State University, Saratov 410012, Russia

ARTICLE INFO

Keywords
Magnetometer
Spin-wave device
Quantum sensor
Noise
Magnons

ABSTRACT

We demonstrate experimentally the operation of a spin-wave magnetometer integrated into a circuit with a positive feedback. The circuit consists of the passive magnetic and active electric parts. The magnetic part includes a sensing element, which is a magnetic cross junction made of $Y_3Fe_2(FeO_4)_3$. The electric part includes a non-linear amplifier and a phase shifter. The electric and magnetic parts are connected via micrometer size antennae. Spin waves are excited by two of these antennae while the output inductive voltage produced by the interfering spin waves is detected by the third antenna. Spin waves propagating in the orthogonal arms of the cross can accumulate significantly different phase shifts, depending on the direction and the strength of the external magnetic field. The output inductive voltage reaches its maximum in the case of constructive spin wave interference. The positive feedback provides further signal amplification. It appears possible to enhance the response function, compared to the passive circuits without a feedback, by a factor of $\times 100$ without an increase in the noise level. The experimental data show a prominent response to the external magnetic field variation, exceeding $5 \times 10^3 V/T$. The intrinsic noise spectral density of the device can be as low as 10^{-16} V^2/Hz. The estimated sensitivity of the prototype device is $2 \times 10^{-12} T/\sqrt{Hz}$ at room temperature. We argue that spin-wave magnetometers can potentially be as sensitive as SQUIDs while operating at room temperature.

1. Introduction

Magnetometers are used in many practical applications including medicine, transportation safety, and homeland security [1–4]. There is a number of different magnetometers, including the superconducting quantum interference devices (SQUIDs) [5], resonance magnetometers, *e.g.* proton magnetometers [6], He^4 e^--spin magnetometers [7], solid-state magnetometers, *e.g.* fluxgate, giant magneto-impedance, magneto-resistive, Hall, magneto-electric [8], and a large variety of the fiber-optic magnetometers [9–11]. Each of the above-mentioned magnetometers possesses some advantages and shortcomings depending on the principle of operation. As for today, the maximum sensitivity, up to atto-Tesla, is provided by SQUIDs [5]. The high sensitivity is critically important in medical applications such as magnetic field imaging (MFI) and magneto-cardiography. However, this high level of sensitivity can be achieved only at the liquid helium temperature of 4 K (−269 °C). The latter explains a strong motivation for developing a magnetometer, which provides the same or better sensitivity than SQUID, while operating at room temperature.

In our preceding work [12], we described a magnetic field sensor based on a spin-wave interferometer without a feedback loop. We reported experimental data obtained for a micrometer-scale $Y_3Fe_2(FeO_4)_3$ cross structure. The maximum recorded response exceeded 40 dB per 1 Oe at room temperature. In this work, we present experimental data for a spin-wave interferometer integrated into a circuit with a positive feedback. The self-exciting positive-feedback spin-wave systems, often termed the spin-wave active rings, are used for the microwave signal generation [13,14]. The ring combines a dispersive spin-wave waveguide with a variable-gain electrical feedback loop. The waveguide and the electric part are connected via a set of the exciting and receiving antennae. The signal amplification occurs when the magnetic and electric parts of the ring are matched [15]. It has been demonstrated in Ref. [16] that a delay line based on a one-dimensional magnonic crystal used in the feedback loop of a microwave auto-oscillator can substantially reduce the phase noise figure and improve other performance characteristics of the auto-oscillator. The design of our magnetometer allows us to exploit all the advantages of the circuits with the positive feedback for enhancing the sensitivity of the spin-wave magnetometers. The rest of the paper is organized as following. In Section II, we describe the principle of operation of the spin-wave magnetometer with a positive feedback. The experimental data on the transfer function and noise characteristics of the prototype device are provided in Section III.

* Corresponding author.
E-mail address: akhitun@engr.ucr.edu (A. Khitun)

https://doi.org/10.1016/j.jmmm.2020.167046
Received 21 February 2020; Received in revised form 2 May 2020; Accepted 19 May 2020
Available online xxx
0304-8853/

The discussion and conclusions are given in Section IV and V, respectively.

2. Principle of operation

A schematic of the spin-wave magnetometer with a positive feedback is shown in Fig. 1. It is an active ring system consisting of the electric and magnetic parts connected in series. The magnetic part is a spin-wave interferometer, which serves as a sensing element to a magnetic field. The core of the sensing element is a magnetic cross junction made of a material with the low spin-wave damping, *e.g.*, YIG, CoFeB or NiFe. There are two input micro-antennae, *i.e.*, marked as 1 and 2, fabricated on the edges of the waveguides. The output antenna, *i.e.*, marked as 3, is located on the other junction. The antennae can be directly placed on top of an insulating material, *e.g.*, YIG, or separated by a layer of insulator from the waveguide in the case of a conducting material, *e.g.* NiFe. The electric part consists of a non-linear amplifier, phase shifter, and an attenuator connected via standard coaxial cables for the RF signal transmission. A connection between the electric and magnetic parts is accomplished by the micro-antennae. An alternating electric current flowing through the input antennae provides an alternating magnetic field, which excites propagating spin waves in the magnetic waveguides. The excited spin waves propagate through the waveguides and interfere in the junction. The interfering spin waves alter the magnetic flux through the output antenna and produce inductive voltage. The details of the spin-wave excitation and detection by micro-antennae can be found elsewhere [17,18].

The entire system constitutes a closed ring circuit where the energy transforms from EM waves in the coaxial cables to the spin waves in magnetic waveguides and vice versa. There is a non-linear electric amplifier in the electric part of the loop. It provides the energy flow in the system. The level of the pumping power is not fixed and it can vary in time, depending on the impedance matching between the parts. For example, the system evolves to the self-oscillation regime, where the pumping power attains its maximum, in the case of impedance matching. The pumping power drops when the two parts are not matched. In its turn, the impedance of the spin-wave interferometer is sensitive to the external magnetic field variation. Thus, the variation of the external magnetic field can be detected by measuring the change of the circulating power.

In general, the dynamics of the active ring system can be described by the equation [15]:

$$L^{-1}(id/dt)\,c(t) - G(p)\,c(t) = \xi(t) \tag{1}$$

where the operator $L(id/dt)$in the frequency domain can be described by a transfer function $L(\omega)$ that is defined as a Fourier transform of the impulse response function of the oscillating system, $c(t)$describes the complex amplitude of the auto-oscillation at the input of the non-linear element, $p = |c(t)|^2$is the signal power, $G(p)$describes the active element, *i.e.* the amplifier, and the function $\xi(t)$ describes the input driving signal acting on the auto-oscillating loop. The theory of the active ring circuits with delayed feedback is described in details in Ref. [15]. The stable limit cycle of the auto-oscillator for the function $c(t)$ has the form:

$$c_s(t) = \sqrt{p_s}e^{-i\phi(t)} \tag{2}$$

where $\phi(t) = \omega_s t + \phi_0$, p_s and ω_s are the stationary free-running auto-oscillation power and frequency, respectively, and ϕ_0 is an arbitrary initial phase of the auto-oscillations. The parameters p_s and ω_s of the stationary auto-oscillation are determined by the amplitude and phase conditions for $\xi(t) = 0$, which follow directly from Eq. (1):

$$\begin{aligned} &\text{abs}\left[L(\omega_s)\,G(p_s)\right] \geq 1 \\ &\arg\left[L(\omega_s)\right] + \arg\left[G(p_s)\right] = 2\pi n \end{aligned} \tag{3}$$

where $n = 1, 2, 3, \ldots$ is an integer number. The first condition defines the minimum level of amplification required to compensate the internal

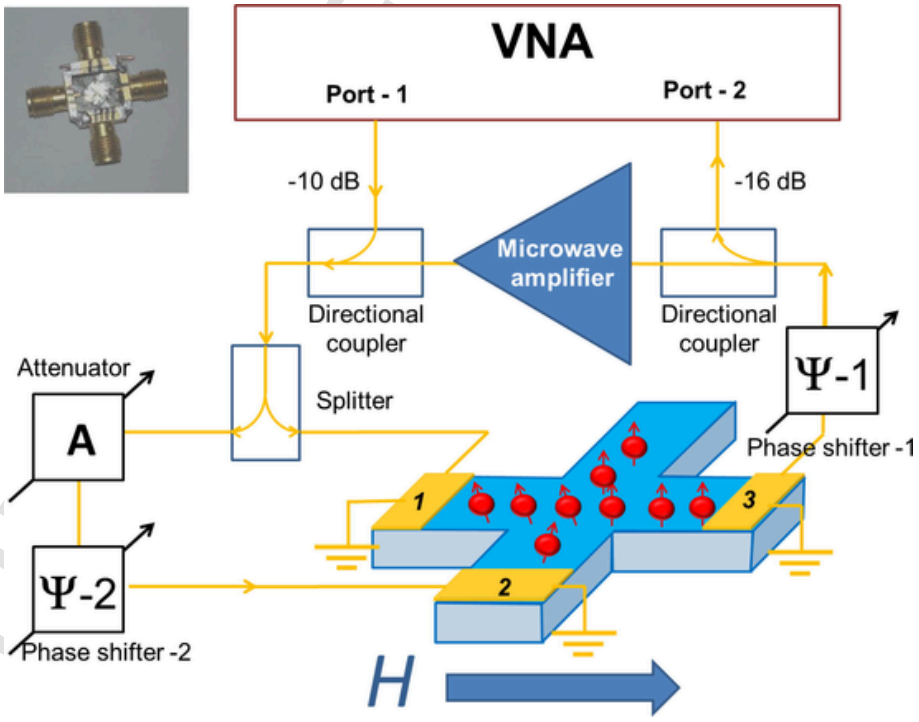

Fig. 1. Schematic of the magnetometer circuit with a positive feedback. It is an active ring system consisting of the electric and magnetic parts connected in series. The sensing element is a magnetic cross junction with micro-antennae fabricated on the edges of the arms. The electric part consists of a non-linear amplifier, phase shifter, and an attenuator connected via standard coaxial cables for RF signal transmission. The connection between the electric and magnetic parts is accomplished by the micro-antennae. The output signal from the magnetometer is collected form antenna No 3 and passed to the VNA. The inset shows a photo of a spin-wave device packaged with four coaxial cables connected to the micro-antennae.

loses in the circuit. Thus, the energy flow provided by the amplifier should exceed the signal attenuation within the spin-wave part and in the connecting cables. The second condition relates the phases accumulated by the propagating signal in the electric and magnetic parts.

The operation of the spin wave magnetometer is based on the dependence of the spin-wave dispersion on the external magnetic field. We restrict our consideration to relatively long-wavelength magneto-static spin waves where the dipole–dipole interaction dominates over the exchange coupling. The dispersion of the magneto-static spin waves depends on the strength as well as the direction of the magnetic field [19]. For example, significantly different phase shifts for the same field may occur for the spin waves propagating perpendicular to the external magnetic field, *i.e.* magneto-static surface spin waves (MSSWs) and the spin waves propagating parallel to the direction of the external field, *i.e.* backward volume magneto-static spin waves (BVMSWs). The ratio of the phase shift, $\Delta\phi$, to the external magnetic field variation, δH, in the ferromagnetic film can be expressed via the equations [20]:

$$\frac{\Delta\varphi}{\delta H} = \frac{l}{d}\frac{(\gamma H)^2+\omega^2}{2\pi\gamma^2 M_S H^2}, k\|H(\mathrm{BVMSW})$$

$$\frac{\Delta\varphi}{\delta H} = \frac{l}{d}\frac{\gamma^2\left(H+2\pi M_S\right)}{\omega^2-\gamma^2(H+2\pi M_S)^2}, k\perp H(\mathrm{MSSW}) \quad (4)$$

Here $\Delta\varphi$ is the phase shift produced by the change in the external magnetic field δH, $l$is the length of the waveguide, d is the thickness of the waveguide, γ is the gyromagnetic ratio, and $4\pi M_s$ is the saturation magnetization of the magnetic material. The formulae above are derived from the dispersion laws of magnetostatic spin waves [21]. In order to maximize the effect of the magnetic field variation on the spin-wave transport, we have previously proposed a spin- wave interferometer based on a magnetic cross junction [12]. There is a relatively narrow window in the frequency domain where BVMSW and MSSW dispersion overlap due to the shape anisotropy of the cross junction [22]. The latter makes it possible to build a spin-wave interferometer based on different types of the spin waves. As it was shown in our preceding work [12] that a small variation in the external magnetic field can strongly affect the interference, resulting in a drastic change in the transmitted spin-wave energy, *i.e.*, 40 dB per 1 Oe, and the output phase, *i.e.* a π-phase shift within 1 Oe. A physical model explaining the difference in the accumulated phases was presented in Ref. [12], and it is not reproduced here. In this work, we treat a magnetic cross junction as a passive non-linear element with the impedance depending on the external magnetic field $L(\omega) \equiv L(H)$. It should be noted that the non-linearity comes from the non-linear spin-wave dispersion rather than from the spin-wave interference, which is a linear process. The utilization of the active ring circuit allows us to drastically enhance the response of the device to the variations in the magnetic field.

We have used the following measurement protocol. Prior to the measuring the signals, the phase shifter Ψ-2 (see Fig. 1) has been adjusted to provide the constructive spin-wave interference in the cross junction. As the next step, the phase shifter Ψ-1 is setup to meet the phase condition of Eq. (3), *e.g.*, the sum of phase shifts in the magnetic and electric parts is $2\pi n$. The gain of the amplifier is set up to be just below the internal loop losses. As a result, both the amplitude and the phase conditions of Eq. (3) are meet for a given bias magnetic field H. The system is most sensitive to the external magnetic field variation in this regime. A tiny variation of the external magnetic field, ΔH, destroys the constructive interference condition for the spin waves, and moves the whole system out of the resonance. Detecting the change in the oscillation amplitude, p, allows one to determine the change in the external magnetic field ΔH. In the next section, we present experimental data, showing the dependence of the oscillation amplitude on the external magnetic field $p(H)$.

3. Experimental data

In our experiments, we utilized a magnetic cross junction, similar to the one used in the preceding work [12]. The cross junction is made of a single crystal YIG film. The film was grown on top of a gadolinium gallium garnet ($Gd_3Ga_5O_{12}$) substrate using the liquid-phase epitaxy technique. The micro-patterning was performed by the laser ablation using a pulsed infrared laser of wavelength $\lambda\approx1.03$ μm, and a pulse duration of ~ 256 ns. The YIG cross has the following dimensions: the length of each waveguide is 3.65 mm, the width is 650 μm, and the YIG film thickness is 3.8 μm. The saturation magnetization of the material was determined to be $4\pi M_0 \approx 1750Oe$ using standard ferromagnetic resonance (FMR) technique. There are four Π-shaped micro-antennae fabricated on the edges of the crosses. The antennae were fabricated from a gold wire of thickness $w = 24.5$ μm. placed directly on top of the YIG surface and fixed at the edges using conductive silver paste. Based on general equations for the spin wave excitation [23,24], one can affirm that such micro-antennae are able to excite and detect spin waves with k-vectors $k \le \pi/w = 1.28 \times 10^3$ cm^{-1}. The device is operating at a certain value of the k-vector in the range of several hundreds of inverse centimeters, which is the same for MSSW and BVMSW [12]. A photo of a packaged device is shown as an inset to Fig. 1. It is a four terminal device with antennae connected to the SMA cables. In the reported experiments only three ports have been used. The device was placed inside an electromagnet (GMW model 3472 – 70) with the pole cap of 50 mm (2 in.) diameter tapered. The system provided a uniform bias magnetic field $\Delta H/H < 10^{-4}$ per 1 mm in the range from – 2000 Oe to + 2000 Oe. Based on the power source specification (KEPCO), the magnetic field instability was estimated about 0.15 Oe. Before the experiment, we determined the region in the frequency-bias magnetic-field space where both types of waves, *i.e.* BVMSW and MSSW, can propagate as described in Ref.[16]. Typically, the most prominent overlap takes place in the frequency range from 4 GHz to 5 GHz, and the bias magnetic field from 750 Oe to 1200 Oe. In this work, we used a bias magnetic field $H = 969$ Oe, which corresponds to the spin-wave frequency $f = 4.38$ GHz. In order to monitor the ring dynamics, a small portion of the active ring power was directed to a programmable network analyzer (PNA Keysight N5241A) via a set of unidirectional couplers (see Fig. 1). The couplers provided −10 dB and −16 dB attenuation, respectively, compared to the signal in the ring circuit.

In Fig. 2, we present experimental data showing the dependence of the output voltage, detected via VNA, on variation of the external mag-

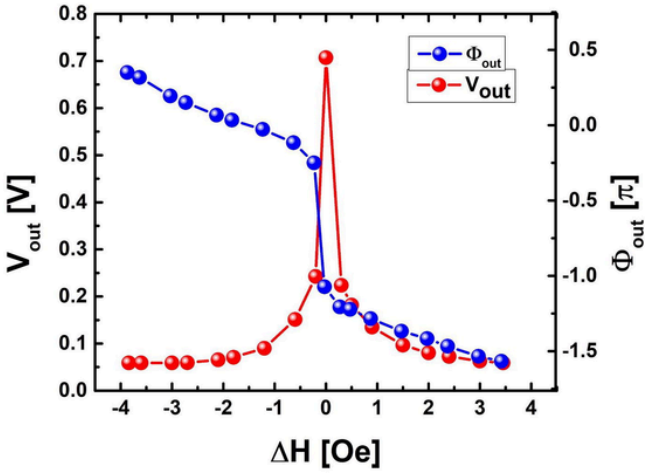

Fig. 2. Experimental data showing the output characteristics as a function of the external magnetic field variation. The amplitude (red curve) and the phase (blue curve) of the inductive voltage detected at the port 3 as a function of the spin-wave phase difference. The output voltage maximum corresponds to the constructive spin-wave interference.

netic field. The red curve depicts the amplitude of the output voltage while the blue curve depicts the phase of the output signal normalized to π. Both the amplitude and the phase of the output signal were measured by VNA via S_{21} parameter. We used an attenuator and a phase shifter to maximize the output voltage at the fixed bias magnetic field $H = 969$ Oe. Next, we varied the magnetic field in the range ± 4 Oe. The observed experimental data show prominent change of the inductive voltage, which reaches 0.72 V in the maximum and drops to 0.05 V in the minimum. The maximum inductive voltage corresponds to the constructive spin-wave interference, resulting to the minimum reflection and maximum transmission through the junction. The voltage drops as the spin-wave interferometer moves out of the constructive interference condition. The latter is well confirmed by the change in the phase of the output signal. The output phase Ψ_{out} is defined as the phase difference between the phases of the ports #1 and #2 of VNA. The data show a π-phase jump in the vicinity of the constructive interference point. A similar behavior was detected in the cross junction without an active ring circuit [12]. The maximum sensitivity to the external magnetic field variation exceeding 0.65 V/1 Oe is observed near the constructive interference point. All measurements have been performed at room temperature.

The intrinsic noise of a sensor is another important parameter characterizing its performance. The noise of the sensor was measured in a following way. The spin waves were excited by the excitation antenna powered by the VNA in the continues wave (CW) operation mode. In order to measure the amplitude fluctuations, a Schottky diode (Keysight Technologies 33330B) was connected to the receiver antenna. The DC detected signal from the diode was amplified by the low noise amplifier (Stanford Research 560) and analyzed by a spectrum analyzer (FFT Photon). As a result, the spectrum of the low-frequency amplitude fluctuations at given RF frequency and power of the excitation was obtained. We excluded the background electronic noise of the detector and RF generator by conducting controlled experiments with the detector connected directly to the VNA output. More details of the measurement procedures for the noise of spin waves can be found in Ref. [25,26]. The normalized noise spectral power density, S_V, obtained in these measurements varied in the interval from 10^{-16} V^2/Hz to 10^{-13} V^2/Hz. The noise level in the entire interval is low, attesting for practical potential of the proposed spin-wave magnetometer with a positive feedback. One should note that the noise level in the considered device can be affected by numerous factors, including temperature fluctuations, power levels, and even local heating induced by interfering waves. Some of the effects of the material parameter fluctuations in YIG waveguides have been addressed previously [27,28]. More studies of the noise at different temperatures and in devices with comparable sizes but different feedback design are needed in order to make definitive conclusions about the ultimate noise levels in such systems.

4. Discussion

The sensitivity of the magnetic sensor is a characteristic which relates the input magnetic field to the output voltage $S_B^V(V/T)$ [4]. The most sensitive sensors show the transfer coefficient as high as 10^5 V/T [4]. Experimental data presented in Fig. 2 demonstrate more than 0.5 V/Oe or 5×10^3 V/T transfer function in the vicinity of the constructive interference point. It is two orders of magnitude larger than the previously reported data 1 mV per 1 Oe [12]. Similar to the previous experiments, the maximum sensitivity is observed for magnetic field directed in-plane with the cross junction along one of the arms. In this case, MSSW and BVMSW propagating in the orthogonal arms accumulate the maximum phase difference.

The intrinsic noise of the sensor $B_n(f)$ is another important characteristic, where f is the frequency. The intrinsic noise is usually estimated by measuring the time variation of the output voltage of the sensor followed by the Fourier transform. The result is divided by the transfer function $S_B^V(V/T)$ leading to $B_{n,eq}(f)$ expressed in $T/\sqrt{Hz}$ [4]. From the measured noise we found that the intrinsic noise of the spin-wave magnetometer attains its maximum under the constructive interference and drops to its minimum in the case of the destructive interference. Combining the transfer function of 5×10^3 V/T and minimum noise level, we obtain an estimate of the spin-wave magnetometer sensitivity to be $2 \times 10^{-12} T/\sqrt{H}$ at room temperature. Note that the experimental data were obtained for a non-optimized prototype device. A better sensitivity to the external magnetic field variation can be achieved by decreasing the thickness of the magnetic waveguides (see Eq. (4)). It is also possible to utilize the second output of the cross junction for the output voltage enhancement. The noise of the spin-wave magnetometer can be further reduced as well. In general, there are two dominant noise sources in the sensing element of the device [25,26,29]. The first one is the noise associated with the propagation of the spin waves. Propagating in the waveguide, the spin waves acquire variations in the amplitude and phase due to the fluctuations of the physical properties of the YIG thin film [25]. The second type if the electronic thermal noise due to the current fluctuations in the conducting antennae. The electronic noise dominates at relatively low input powers while the spin wave noise becomes observable at relatively high input powers. In our noise measurements, we tested the regime of the high input power (18 dBm), which is close to the four-magnon instability threshold [25]. For this reason, designing smaller devices with higher quality materials and operating them at lower power can potentially lead to even lower noise levels. The effect of noise suppression in magnonic system with positive feedback was reported by other groups [30]. The later shows an additional possibility for noise reduction while increasing the transfer function.

5. Conclusions

We designed and experimentally demonstrated a spin-wave magnetometer with a positive feedback. Experimental data show prominent response to external magnetic field variation exceeding 5×10^3 V/T. The intrinsic noise spectral density of the device can be as low as 10^{-16} V^2/Hz. The spin-wave magnetometer sensitivity was estimated to be $2 \times 10^{-12} T/\sqrt{H}$ at room temperature. The utilization of the circuit with a positive feedback made it possible to strongly enhance the sensitivity to the magnetic field variation compared to the previously reported devices with the passive configuration. The demonstrated prototype devices were based on YIG micrometer thick structures to ensure sufficiently long spin wave coherent length at room temperature. The feasibility of using other magnetic materials, reproducibility, and stability are important practical questions to be student in the future works. Potentially, the spin wave magnetometers can be placed on permanent magnet providing a stable bias field up to 1 T. Physical considerations indicate that the intrinsic noise can be reduced further in smaller scale devices with higher quality material, operating at lower power levels. The proposed spin-wave magnetometers can potentially compete with SQUIDs in sensitivity while operating at room temperature.

Acknowledgements

The work at UCR was supported, in part, by the Spins and Heat in Nanoscale Electronic Systems (SHINES), an Energy Frontier Research Center funded by the U.S. Department of Energy, Office of Science, Basic Energy Sciences (BES) under Award # SC0012670. The work of A. Kozhevnikov and Y. Filimonov was supported by Russian Science Foundation grant №17-19-01673. The authors are indebted to Professor Sergey Rumyantsev (UCR; current affiliation Center for Terahertz Research and Applications, Polish Academy of Sciences) for his help with the measurements and data analysis.

Appendix A. Supplementary data

Supplementary data to this article can be found online at https://doi.org/10.1016/j.jmmm.2020.167046.

References

[1] H P Baltes, R S Popovic, Integrated semiconductor magnetic-field sensors, Proc. IEEE 74 (1986) 1107–1132, doi:10.1109/proc.1986.13597.
[2] J Heremans, Solid-state magnetic-field sensors and applications, J. Phys. D-Appl. Phys. 26 (1993) 1149–1168, doi:10.1088/0022-3727/26/8/001.
[3] S Kordic, Integrated silicon magnetic-field sensors, Sensors Actuators 10 (1986) 347–378, doi:10.1016/0250-6874(86)80054-3.
[4] D Robbes, Highly sensitive magnetometers - a review, Sensors Actuators a-Phys. 129 (2006) 86–93, doi:10.1016/j.sna.2005.11.023.
[5] W. Tao, J. Gao, F. Zhang, W. Cai, and P. Deng, High-Tc squid sensors and its application in bio-magnetic measurement, 2012.
[6] S Begus, D Fefer, An absorption-type proton NMR magnetometer for measuring low magnetic fields, Measure. Sci. Technol. 18 (2007) 901–906, doi:10.1088/0957-0233/18/3/045.
[7] A Nikiel, P Bluemler, W Heil, M Hehn, S Karpuk, A Maul, E Otten, L M Schreiber, M Terekhov, Ultrasensitive He-3 magnetometer for measurements of high magnetic fields, Eur. Phys. J. D 68 (2014) DOI: 33010.1140/epjd/e2014-50401-3.
[8] P. Ripka, Magnetic sensors and magnetometers - Preface, 2001.
[9] G W Day, Recent advances in Faraday effect sensors, Optical Fiber Sensors, Springer-Verlag, Berlin, West Germany, 1989, pp. 250–254.
[10] H Okamura, Fiber-optic magnetic sensor utilizing the Lorentzian force, J. Lightwave Technol. 8 (1990) 1558–1564.
[11] K P Koo, F Bucholtz, D M Dagenais, A Dandridge, A compact fiber-optic magnetometer employing an amorphous metal wire transducer, IEEE Photon. Technol. Lett. 1 (1989) 464–466.
[12] M Balynsky, D Gutierrez, H Chiang, A Kozhevnikov, G Dudko, Y Filimonov, A A Balandin, A Khitun, A magnetometer based on a spin wave interferometer, Sci. Rep. 7 (2017) 1–11, doi:10.1038/s41598-017-11881-y.
[13] B A Kalinikos, N G Kovshikov, C E Patton, Self-generation of microwave magnetic envelope soliton trains in yttrium iron garnet thin films, Phys. Rev. Lett. 80 (1998) 4301–4304, doi:10.1103/PhysRevLett.80.4301.
[14] S O Demokritov, A A Serga, V E Demidov, B Hillebrands, M P Kostylev, B A Kalinikos, Experimental observation of symmetry-breaking nonlinear modes in an active ring, Nature 426 (Nov 2003) 159–162, doi:10.1038/nature02042.
[15] V S Tiberkevich, R S Khymyn, H X Tang, A N Slavin, Sensitivity to external signals and synchronization properties of a non-isochronous auto-oscillator with delayed feedback, Sci. Rep. 4 (2014), doi:10.1038/srep03873.
[16] E Bankowski, T Meitzler, R S Khymyn, V S Tiberkevich, A N Slavin, H X Tang, Magnonic crystal as a delay line for low-noise auto-oscillators, Appl. Phys. Lett. 107 (2015), doi:10.1063/1.4931758.
[17] T J Silva, C S Lee, T M Crawford, C T Rogers, Inductive measurement of ultrafast magnetization dynamics in thin-film Permalloy, J. Appl. Phys. 85 (1999) 7849–7862, doi:10.1063/1.370596.
[18] M Covington, T M Crawford, G J Parker, Time-resolved measurement of propagating spin waves in ferromagnetic thin films, Phys. Rev. Lett. 89 (23) (2002), doi:10.1103/PhysRevLett.89.237202.
[19] A G Gurevich, G A Melkov, Magnetization Oscillations and Waves, CRC Press, 1996.
[20] M P Kostylev, A A Serga, T Schneider, B Leven, B Hillebrands, Spin-wave logical gates, Appl. Phys. Lett. 87 (15) (2005) 153501, doi:10.1063/1.2089147.
[21] S O Demokritov, A A Serga, A André, V E Demidov, M P Kostylev, B Hillebrands, A N Slavin, Tunneling of dipolar spin waves through a region of inhomogeneous magnetic field, Phys. Rev. Lett. 93 (4) (2004), doi:10.1103/PhysRevLett.93.047201.
[22] M Balinskiy, D Gutierrez, H Chiang, Y Filimonov, A Kozhevnikov, A Khitun, Spin wave interference in YIG cross junction, AIP Adv. 7 (5) (2017) 56633, doi:10.1063/1.4974526.
[23] Ganguly A.K. and W. D.C., "Microstrip Excitation of Magnetostatic Surface Waves: Theory and Experiment " IEEE Trans. on MTT, vol. 23, pp. 998-1006, 1975
[24] Sethares J.C. and W. I. J., "Theory of MSW Transducers," Circuits Systems Signal Process, vol. 4, pp. 41-62, 1985
[25] S Rumyantsev, M Balinskiy, F Kargar, A Khitun, A A Balandin, The discrete noise of magnons, Appl. Phys. Lett. 114 (2019), doi:10.1063/1.5088651.
[26] Rumyantsev S., Balinskiy M., Kargar F., Khitun A., and B. A.A., "Low-frequency noise of magnons," in Proceed. of the 25th International Conference on Noise and Fluctuations (ICNF 2019), Neuchâtel, Switzerland, 2019.
[27] Carter R.L., Owens J.M., and D. D.K., "YIG Oscillators: Is a Planar Geometry Better," IEEE Transactions on Microwave Theory and Techniques, vol. 32, pp. 1671-1674, 1984
[28] Drozdovskii A.V. and U. A.B., "Phase noise management of spin-wave delay-line oscillators," Journal of Physics: Conference Series vol. 661, p. 012062, 2015. DOI: doi:10.1088/1742-6596/661/1/012062
[29] "For general background on various types of noise see Balandin, A. A. Noise and Fluctuations Control in Electronic Devices (American Scientific Publishers, Los Angeles, California, USA, 2002).".
[30] Ustinov A.B., Nikitin A.A., and K. B.A., "Electronically tunable spin-wave optoelectronic microwave oscillator," Technical Physics, vol. 60, pp. 1392-1396, 2015. DOI: DOI: 10.1134/S1063784215090224